Paper:

Automatic Counting Robot Development Supporting Qualitative Asbestos Analysis – Asbestos, Air Bubbles, and Particles Classification Using Machine Learning –

Kenichi Ishizu[*1], **Hiroshi Takemura**[*1,*2], **Kuniaki Kawabata**[*2], **Hajime Asama**[*2,*3], **Taketoshi Mishima**[*2,*3,*4], **and Hiroshi Mizoguchi**[*1,*2]

[*1]Faculty of Science and Technology, Tokyo University of Science
2641 Yamazaki, Noda, Chiba 278-8510, Japan
E-mail: {j7508603@ed, takemura@rs}.noda.tus.ac.jp
[*2]Kawabata Intelligent System Research Unit, RIKEN
[*3]RACE, The University of Tokyo
[*4]Department of Information and Computer Science, Saitama University
[Received December 20, 2009; accepted April 22, 2010]

Asbestos, particle, and air bubble counting generally supports qualitative asbestos analysis, using such procedures as dispersion staining. Operators conventionally check and count asbestos fibers visually using a microscope – a difficult, time-consuming process. The microscopic observation robot we are automating to support qualitative asbestos analysis images fibers and saves them automatically to a database. In this paper, we introduce image processing method using machine learning to count asbestos, particles, and air bubbles automatically.

Keywords: asbestos, microscopic observation, qualitative analysis, machine learning

1. Introduction

With asbestos exposure now a huge social issue as a cause of pneumoconiosis and malignant mesothelioma due to previous widespread use as thermal insulation, in fire-retardant material, etc., asbestos deaths are expected to exceed 100,000 in Japan in the next 4 decades [1]. The major threat lies in thermal insulation materials, which require asbestos inclusion analysis in such fields as building demolition.

Japanese Industrial Standards (JIS) strictly define asbestos inclusion analysis procedures in JIS A1481 [2], dividing them into quantitative and qualitative analysis. Quantitative analysis has been speed up thanks to advances in X-ray diffraction and automation. Qualitative analysis, however, has not yet been automated. A qualitative analysis procedure called dispersion staining, which uses phase contrast microscopy to counts asbestos crystals, is currently done visually by operators, putting a heavy burden on them. Worldwide standards stricter than those in Japan have been set, for example, by the United States Environmental Protection Agency (EPA) standards. The demand for asbestos inspection is expected to grow as the number of buildings using asbestos and reaching the end of their usefulness grows, raising the need or efficient, automated asbestos analysis.

With the objective of developing an automatic "asbestos counting" robot supporting qualitative asbestos analysis, we propose automated visual counting using image processing. Part of this involves extracting particles from microscope images and classifying them into asbestos, particle, and bubble images.

2. Dispersion Staining and Problems

Asbestos crystals mixed with other general particles are difficult to recognize and count them. Dispersion staining (JIS A1481) involves counting asbestos crystals using a phase contrast dispersion microscope. That enables asbestos crystal color alone to be changed using the microscope's polarization plate. Operators use asbestos crystal color change to count crystals as strictly defined by JIS. Operators first count 3,000 particles from all particles in the field of view, including asbestos crystals, then count the number of asbestos crystals. A sample of 3,000 particles containing 4 or more asbestos crystals is judged to be inclusive. Counting is done currently done visually, requiring long observation time through a microscope, placing a very heavy temporal, physical, and mental burden on operators. Individual operators can examine only about 10 specimens a day, limiting the efficiency of inclusion analysis.

3. Related Studies

The many attempts at automating asbestos analysis have included Magiscan [3, 4] and asbestos fibers auto-

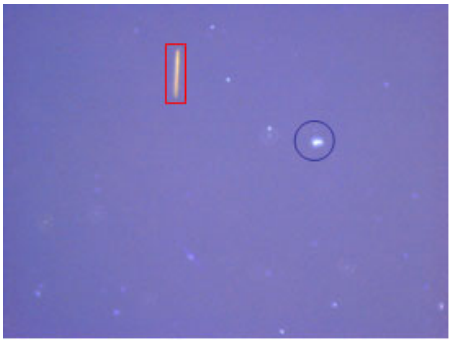

Fig. 1. Microscope image: rectangle indicating asbestos fiber, circle indicating air bubble, and other small bright areas indicating particles.

matic counting [5], which focus on counting asbestos crystals in the air, i.e., only particles filtered and selected are inspected. With particles as large as asbestos crystals in air less likely to be mixed in and small particles filtered out, asbestos crystals are easy to recognize. Samples such as building materials, however, are difficult to search for asbestos crystals, so this study requires differentiating general particles and asbestos crystals.

To automate dispersion staining, Kawabata et al. developed a robot that automatically captures microscopic images [6] while automatically changing polarization, achieving automation. The problem remaining is to refine image capture, which requires automatically counting particles and asbestos crystals in captured images.

Particle detection in dispersion staining includes using background subtraction and Gaussian noise filtering (Kumagai et al. [7]), in which optimal resolution with particle variable inspection is selected based on particle resolution dependence (Watanabe et al. [8]), and using a One Class Support Vector Machine (OCSVM) (Kuba et al. [9]). Asbestos detection in dispersion staining includes a two-class problem of whether asbestos particles are contained in individual local regions of microscope images, solved using an SVM (Nomoto et al. [10]), and particle location displacement in which polarization is changed in dispersion staining using Scale Invariant Feature Transform (SIFT) features to determine whether asbestos is present based on two images (Moriguchi et al. [11]). In dispersion staining, these types of detection handle only particle detection or asbestos detection and not both. The many bubbles in the specimens are also not considered.

4. Automatic Counting

To support operators, particles in microscope images must be classified into asbestos crystals as separate from other general particles. Most images have air mixed in while specimens are prepared, and such air appears as bubbles, as shown in **Fig. 1**. (Red rectangles are asbestos, blue circles bubbles, and other small bright regions all particles (about 30).) Since a bubble must not be counted as a particle, bubbles must be clearly classified. Operators count while classifying items based on experience. We use classification here based on three processes to approach operator counting as closely as possible – particle extraction, asbestos classification, and bubble classification.

5. Particle Extraction

Background subtraction and edge detection are used for particle detection preprocessing. In dispersion staining discussed here, however, microscope image background brightness and color vary greatly with imaging conditions, meaning background images are not constant, and 50 or more images must be processed to count $3,000$ particles, so we must prepare a corresponding number of background images. Asbestos crystals and particles similar in color to the background may not be always detected. Asbestos crystals and particles come in all different colors, sizes, and shapes, too, so applying methods such as template matching is not practical.

Operators recognize and count particles flexibly regardless of color and brightness differences in the background, relying on their experience to spot microscope images background "uniformity." Specifically, they are considered to recognize simple, uniform regions as background regions and other regions as particles. Here, we use operator recognition to automatically classify background from an image, then use a method to extract particles, which vary greatly in size. Extremely small particles not recognized unless the image is enlarged, for example, may be processed as noise and left out. We therefore propose dividing images up into smaller regions.

Particles are counted using a 630×480 pixel image captured in phase contrast microscopy. We divided images into 336 30×30 pixel regions and defined small regions with the particles as small particle regions and those without particles as small background regions. We then obtained all RGB pixel values in small regions and rendered them as pixel values in RGB space. As a result, pixel values distributed widely in the small particle regions, as shown in **Fig. 2**, while they did not distribute widely in the small background regions as shown in **Fig. 3**. We then classified the background using these features.

Pixel variations in RGB space are quantified by calculating variation values, which are an index of how a sample deviates from the sample mean. We calculate the variation of each RGB value in small regions and render the result as a three-dimensional (3D) RGB graph as shown in **Fig. 4**. The graph indicates that each RGB value is small in small background regions (◯), while RGB variation values are large in small particle regions (■). Small regions are thus classified into small background regions and small particle regions by the magnitude of variation.

Particles cannot be extracted and counted by simply classifying small particle and background regions, so we extract particles in a second processing step using information on background regions classified above, as fol-

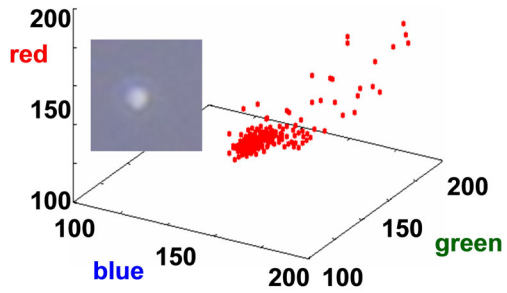

Fig. 2. Small particle region.

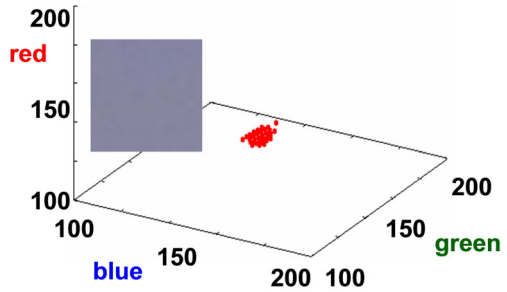

Fig. 3. Small background regions.

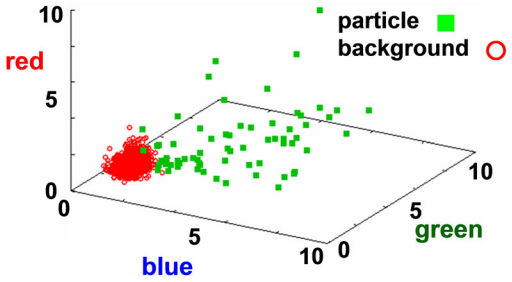

Fig. 4. RGB variation distribution.

lows:

I. Read a phase contrast microscopy image as shown in **Fig. 5(a)**.

II. Determine the mean of R, G, and B in all the small background regions (black in **Fig. 5(b)**) classified using above.

III. Conduct background subtraction in small particle regions with monochromatic backgrounds using the mean of the R, G, and B values determined in II as an example, as shown in **Fig. 5(c)**.

IV. Binarize the image.

V. Conduct labeling.

VI. Box individual extracted particles regions as shown in **Fig. 5(d)**.

VII. Count the result.

Conducting a particle counting experiment as shown above, we used a standard specimen used on site and captured 15 images using Nikon ECIPSE 80i phase contrast microscopy. We had an actual asbestos particle counter count particles in images, compared the result to our processing result, and evaluated them. We compared also

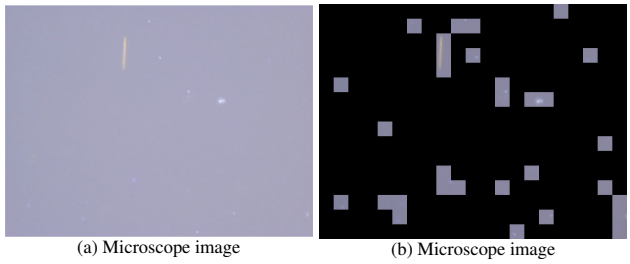

(a) Microscope image (b) Microscope image

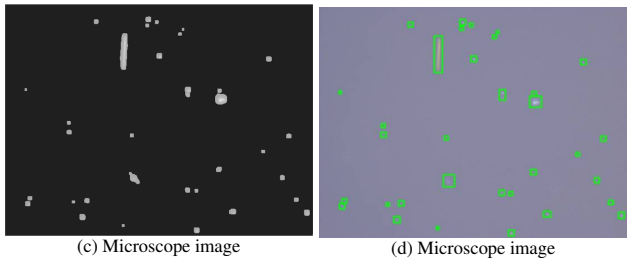

(c) Microscope image (d) Microscope image

Fig. 5. Procedures and results.

Table 1. Particle counting results.

Operator	Proposed method	Correct counting rate	False positive	False negative
540	549	101.7%	13.1%	6.1%

the result with a result with the same image using only background subtraction with a standard background image (in which a prepared slide containing immersion liquid before the specimen was set is captured with the microscope). We compared the counting result of the 15 images of the operator with that of the proposed method as shown in **Table 1**. The operator counted 540 particles and the proposed method counted 549. The extraction rate was 101.7%, the false-positive rate (the proposal detects particles the operator did not extract) 13.1%, and the false-negative rate (the proposal left out particles the operator extracted) 6.1%. The proposed method left out particles mainly because it counted two or more neighboring or overlapping particles as one particle that the operator counted as multiple particles.

We verified each of the 15 images for the result of the proposed method and that using only background subtraction in the standard background, finding that the experiment using only background subtraction has a wide variation in extraction. The proposed method, however, achieved $\pm 10\%$ in 12 of the 15 images, a small variation in extraction among images. Despite a slight image-dependent difference in brightness, we achieved a highly accurate result because classification of background region in particle counting preprocessing functioned well.

We developed a particle detector based on two-step processing: specification of the background region using color variation and particles extraction using information on the background. We also made highly accurate particle counting possible regardless of changes in brightness and color by specifying background region as preprocessing and creating an exemplary background for each image, successfully reducing variation in extraction for each image.

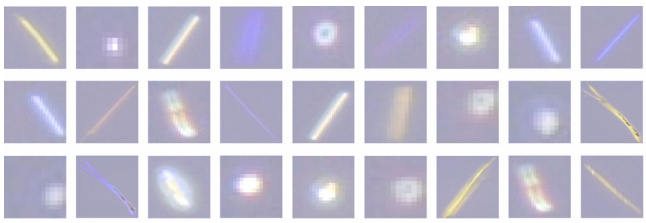

Fig. 6. Example of extracted particles.

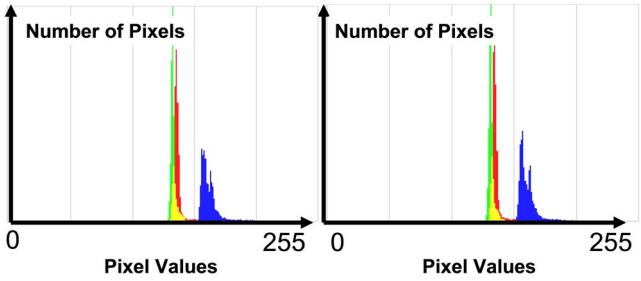

Fig. 7. Particle image histogram.

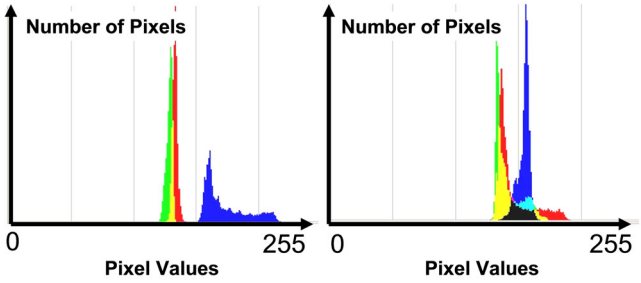

Fig. 8. Asbestos image histogram.

6. Asbestos Classification

We now classify extracted particles, as shown in **Fig. 6**, into asbestos crystals and general particles and count them. Operators use dispersion staining in general to highlight asbestos crystals and count them. In the same way as operators, we use dispersion staining to classify asbestos crystals and particles.

In dispersion staining, particle locations in an image are displaced if polarization changes, so only a simple comparison of images before and after polarization is changed cannot extract asbestos crystals. If particles are extracted from images before and after polarization is changed, it becomes very difficult to associate them, and displacement direction and size depend on images. We extract particles from image A, as a standard, by particle extraction and clip regions having the same coordinates as those of extracted regions from image B, in which polarization has been changed. We verify only the change in color by preparing extracted images of the same size, then compare histograms of images extracted from images A and B to classify asbestos crystal and particle images as shown in **Figs. 7** and **8**. These histograms differ slightly for images A and B. Histograms of asbestos crystal images, in contrast, exhibit great differences between images A and B, and we classify them by calculating and comparing means of their RGB pixels. Assuming that an RGB pixel is a 3D vector, we classify them by images A and B neighborhood degree, determined by calculating the angle formed by

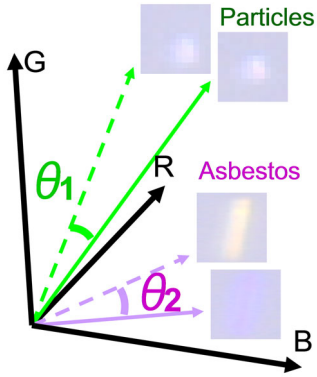

Fig. 9. RGB pixel differences.

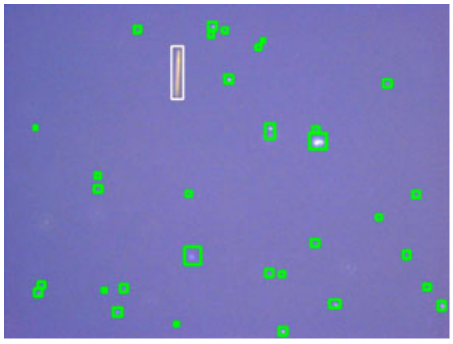

Fig. 10. Asbestos imaging classification. White rectangle: asbestos; green rectangle: particles and air bubble.

vectors of images A and B before classification as shown in **Fig. 9**, thus achieving robust classification less susceptible to brightness and calculating individual angles as follows:

$$Angle = \cos^{-1}\left(\frac{(\text{Average of image}:A)\bullet(\text{Average of image}:B)}{\sqrt{(\text{Average of image}:A)^2(\text{Average of image}:B)^2}}\right) \quad (1)$$

Asbestos crystals are actually classified as follows:

I. Prepare microscope images.

II. Extract particles.

III. Extract from image B the same region as the particle region extracted from image A.

IV. Remove particles less than 20 pixels in size.

V. Calculate means of RGB pixels of images A and B.

VI. Calculate the angle formed by RGB vectors assuming that RGB pixel values determined in V. are vectors.

VII. Classify them into asbestos crystals and other particles by threshold processing based on the calculated angle shown in **Fig. 10**.

We applied classification and conducted experiments on asbestos crystals, using 50 microscopic images of

Table 2. Asbestos experiment classification results.

Particle : 2423	
Correct classification	2383 (98.3%)
False classification	40 (1.7%)
Asbestos : 136	
Correct classification	116 (85.3%)
False classification	20 (14.7%)

Oversight of the asbestos crystal in particle extraction processing： 5

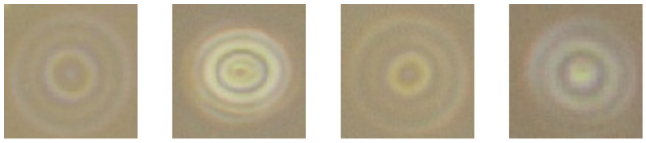

Fig. 11. Example of bubble images.

Fig. 12. Example of particle images.

Fig. 13. Bubble images after edge extraction.

Fig. 14. Example of particle images.

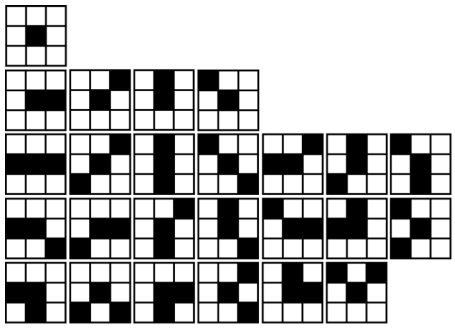

Fig. 15. HLAC features.

Amosite, a type of asbestos. An expert operator operated counting in advance, and we compared counting results to our results to verify the accuracy of the proposed method. Images contain 2,423 particles extracted by the expert operator, among which 136 were recognized as asbestos crystals by the operator. In results for the proposed method, 116 asbestos crystals were discriminated correctly, 40 particles recognized incorrectly as asbestos, and 20 asbestos crystals falsely recognized as other particles. Five asbestos crystals were left out in the particle extraction stage as shown in **Table 2**. This example evaluates classification accuracy, so the five particles left out in preprocessing are excluded from results in the table.

7. Bubble Classification

Particle images extracted by particle extraction contain bubble images as shown in **Figs. 11** and **12**. In particle counting, the operator recognizes bubbles and counts them out, so highly accurate particle counting requires classifying bubble images from general particles. We propose automatically classifying bubbles separately from extracted particle images.

A. Bubble Classification Using Shape

Using bubble shape, since bubbles generally vary in color, shape, and size, we classify them focusing on concentric shape – one factor operators use in recognizing bubbles. To extract concentric shape, we use vertical and horizontal Sobel filters to enhance edges and create binary feature images from which noise is removed by expansion and contraction as shown in **Figs. 13** and **14**.

B. Higher-Order Local Autocorrelation Features

To classify these created feature images, we use the Higher-order Local Autocorrelation (HLAC) [12] – basic image features effective in image recognition and measurement and providing location invariance, i.e., features are invariant for target location, and additivity, i.e., all features are the sum of target features, and model-free, i.e., no target model is assumed [13]. These features are appropriate for classifying bubble images not having a definite shape.

Otsu et al. proposed HLAC features having a feature quantity obtained by extending an autocorrelation function to a higher order and applying it to an image. They integrated features obtained with multivariate data analysis and proposed image measurement and recognition to extract more effective features. Autocorrelation extension is called a higher-order autocorrelation feature. Assuming that target image brightness at reference point r is $I(r)$, the N-th autocorrelation function is defined as follows:

$$x(a_1,\ldots,a_N) = \int I(r)I(r+a_1)\ldots I(r+a_N)dr \quad (2)$$

for N displacements $(a_1,\ldots,a_N)$ around the reference point. Numerous higher-order autocorrelation functions can be assumed based on degree N and displacement direction $(a_1,\ldots,a_N)$, so we limit degree N to 2. In an image, a correlation between neighboring points is usually more important than that between separated points, so we limit the displacement direction to a 3×3 region. The 25 features obtained by a local pattern, as shown in **Fig. 15**, are called HLAC features. We conduct classification using HLAC features obtained by binary bubble images.

Using 75 bubble images and 3,381 particle images, we conducted extraction using HLAC features. The distri-

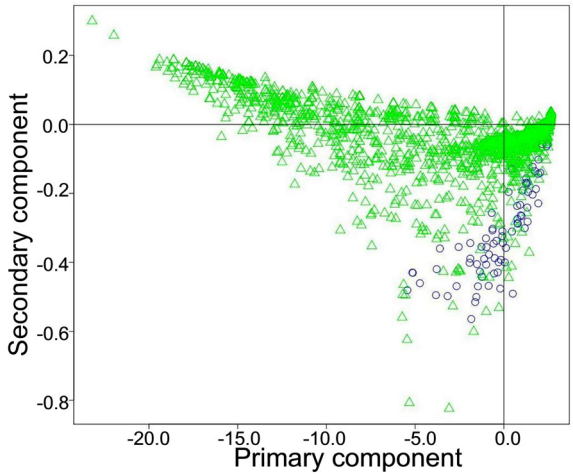

Fig. 16. Particle and air bubble distribution.

bution of 25-dimensional features for each image in feature space is shown in **Fig. 16**. For visualization, 25-dimensional feature space was compressed into two dimensions using principal component analysis. The green triangle is a particle and the blue circle a bubble, showing that particles and bubbles tend to be distributed differently, so HLAC features are considered effective in classification using an appropriate classification method.

C. Support Vector Machine (SVM)

HLAC features from each image are basic general features independent of the recognition target. Information required to recognize a whole is considered extracted. We use HLAC features as learning data to classify extracted 25-dimensional features into classes – bubbles or general particles. We conduct classification using a Support Vector Machine (SVM), commonly used to recognize targets with high degrees of freedom such as scenes and landscapes [14].

Numerous classification hyperplanes separate two classes in linear discriminants. The SVM introduces a discrimination using a margin concept. When linear separation is difficult, separation is made possible by mapping learning data onto higher-order space. The SVM algorithm uses only the inner product between feature vectors, so a nonlinear discrimination function is constructed using a kernel trick replacing the inner product with any kernel function, i.e., in this paper, a polynomial kernel, empirically determining each parameter. The image is 70×70 pixels.

D. Classification Experiments

We conducted classification experiments to verify the feasibility of bubble classification, preparing 75 bubble images and 3,381 particle images actually extracted from microscope images, from which we used 30 bubble images and 50 particle images selected randomly as images for the teacher and remaining 45 bubble images and 3331 particle images as images for testing. Classification resulted in a high success of 95.6% in correct classification for bubbles and of 97.5 for particles, as shown in **Table 3**.

Table 3. Air bubble classification experiment results.

Particle : 3331	
Correct classification	3248 (97.5%)
False classification	83 (2.5%)
Air Bubble:45	
Correct classification	43 (95.6%)
False classification	22 (4.4%)

8. Conclusions

To support qualitative asbestos particle analysis, we have enabled operators to conduct visual analysis using image processing using particle extraction, asbestos classification, and bubble classification. Particle extraction enabled highly accurate background-based extraction. Asbestos classification was achieved using changes in asbestos crystal color, which is a feature of dispersion staining. Bubbles and general particles were classified using bubble shape and HLAC features and an SVM. Our study's eventual objective is to develop a robot supporting qualitative asbestos analysis – a socially significant goal.

Acknowledgements

This study was implemented under a Grant-in-Aid for Scientific Research on Waste Disposal from the Ministry of the Environment of Japan.

References:

[1] T. Murakami, "A study of quantitative prediction of asbestos pollution risks for the future," Research on Environmental Disruption, Vol.32, pp. 31-38, 2002. (in Japanese)
[2] JIS (Japanese Industrial Standard) A1481,2006(J), "Determination of Asbestos in Building Material Products," 2006.
[3] L. C. Kenny, "Asbestos fibre counting by image analysis – the performance of Manchester asbestos program on Magiscan," Anm Occup Hyg, Vol.28, No.4, pp. 401-415, 1984.
[4] P. A. Baron and S. A. Shulman, "Evaluation of the Magiscan image analyzer for asbestos fiber counting," Am Ind Hyg Assoc J., Vol.48, No.1, pp. 39-46, 1987.
[5] Y. Inoue, A. Kaga, K. Yamaguchi, "Development of an automatic system for counting asbestos fibers using image processing," Paticul Sci Technol, Vol.16, No.4, pp. 263-279, 1998.
[6] K. Kawabata, S. Morishita, H. Takemura, K. Hotta, T. Mishima, H. Asama, H. Mizoguchi, and H. Takahashi, "Development of an Automated Microscope for Supporting Qualitative Asbestos Analysis by Dispersion Staining," J. of Robotics and Mechatronics, Vol.21, No.2, pp. 186-192,2009.
[7] H. Kumagai, S. Morishita, K. Kawabata, H. Asama, and T. Mishima, "Accuracy Improvement of Counting Asbestos in Particles using a Noise Redacted Background Subtraction," Proc. of IEEE Int. Conf. on Multisensor Fusion and Integration for Intelligent Systems, pp. 74-79, 2008.
[8] T. Watanabe, S. Morishita, K. Kawabata, H. Asama, and T. Mishima, "Resolution Dependency of a Particle Detection Method in Microscopy Images for Asbestos Qualitative Analysis," SSI2008, pp. 319-322, 2008. (in Japanese)
[9] H. Kuba, K. Hotta, and H. Takahashi, "Automatic Particle Detection and Counting By One-Class SVM From Microscope Image," Proc. of Int. Conf. on Neural Information Processing, pp. 361-368, 2008.
[10] A. Nomoto, K. Hotta, and H. Takahashi, "An Asbestos Counting Method from Microscope Image of Building Materials Using Summation Kernel of Color and Shape," Proc. of Int. Conf. on Neural Information Processing, pp. 671-678, 2008.
[11] Y. Moriguchi, K. Hotta, and H. Takahashi, "An Asbestos Detection Method From Microscope Image Using Support Vector Random Field of Local Color Features," IEEJ Trans. EIS, Vol.129, No.5, pp. 818-823, 2009.

[12] J. A. Mclaughlin and J. Raviv, "*N*-th-order autocorrelations in pattern recognition," Information and Control, Vol.12, pp. 121-142, 1968.
[13] N. Otsu and T. Kurita, "A new scheme for practical flexible and intelligent vision systems," Proc. IAPR Workshop on Computer Vision, pp.431-435, 1988.
[14] V. N. Vapnik, "An overview of statistical learning theory," Neural Networks, IEEE Trans. on, Vol.10, No.5, pp. 988-999, 1999.

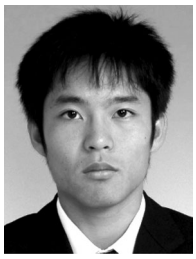

Name:
Kenichi Ishizu

Affiliation:
Student, Graduate School of Science and Technology, Tokyo University of Science

Address:
2641 Yamazaki, Noda, Chiba 278-8510, Japan

Brief Biographical History:
2008 Received B.S. degree in Mechanical Engineering from Tokyo University of Science

Main Works:
• K. Ishizu, H. Takemura, K. Kawabata, H. Asama, T. Mishima, and H. Mizoguchi, "Image Processing of Particle Detection for Asbestos Qualitative Analysis Support Method – Particle Counting System based on Classification of Background Area –," Proc. of ICARCV2008, pp. 868-873, 2008.

Membership in Academic Societies:
• The Japan Society of Mechanical Engineers (JSME)

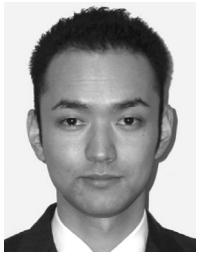

Name:
Hiroshi Takemura

Affiliation:
Junior Associate Professor, Department of Mechanical Engineering, Tokyo University of Science

Address:
2641 Yamazaki, Noda, Chiba 278-8510, Japan

Brief Biographical History:
2004- Guest Lecturer of Industrial Applications of Computer Science and Micro Systems, Universitat Karlsruhe
2005- Assistant Professor of the Department of Mechanical Engineering, Tokyo University of Science
2007- Visiting Researcher of RIKEN (The Institute of Physical and Chemical Research)
2008- Visiting Scholar of the Department of Mechanical Engineering, University of Michigan
2010- Junior Associate Professor of the Department of Mechanical Engineering, Tokyo University of Science

Main Works:
• "Slip-adaptive Walk of Quadruped Robot," Journal of Robotics and Autonomous Systems, Vol.53, No.2, pp. 124-141, 2005.

Membership in Academic Societies:
• Institute of Electrical and Electronics Engineers, Inc. (IEEE)
• The Japan Society of Mechanical Engineers (JSME)
• The Robotics Society of Japan (RSJ)

Name:
Kuniaki Kawabata

Affiliation:
Senior Research Scientist, Molecular & Informative Life Science Unit, RIKEN (The Institute of Physical and Chemical Research)

Address:
2-1 Hirosawa, Wako, Saitama 351-0198, Japan

Brief Biographical History:
1997- Joined Biochemical Systems Lab. at RIKEN as a Special Postdoctoral Researcher
2000- Joined Advanced Engineering Center at RIKEN as a Research Scientist
2002- Joined to Distributed Adaptive Robotics Research Unit, RIKEN
2005- Unit Leader of Distributed Adaptive Robotics Research Unit, RIKEN
2007- Unit Leader of Intelligent System Research Unit, RIKEN
2010- Senior Research Scientist, Molecular & Informative Life Science Unit, RIKEN

Main Works:
• distributed autonomous robotic systems, intelligent ubiquitous information device, machine learning, visual perception

Membership in Academic Societies:
• The Japan Society of Mechanical Engineers (JSME)
• The Robotics Society of Japan (RSJ)
• The Japanese Society of Instrumentation and Control Engineers (SICE)
• Institute of Electrical and Electronics Engineers, Inc. (IEEE)

Name:
Hajime Asama

Affiliation:
Department of Precision Engineering, School of Engineering, The University of Tokyo

Address:
7-3-1 Hongo, Bunkyo-ku, Tokyo 113-8656, Japan

Brief Biographical History:
1986- Research Associate of RIKEN (The Institute of Physical and Chemical Research)
1998- Professor, RACE (Research into Artifacts, Center for Engineering), The University of Tokyo
2002- Professor, Department of Precision Engineering, School of Engineering, The University of Tokyo

Main Works:
• D. Chugo, K. Kawabata, H. Kaetsu, H. Asama, and T. Mishima, "Omni-directional Vehicle Control Based on Body Configuration," Industrial Robot, Vol.36, No.5, pp. 461-468, 2009.

Membership in Academic Societies:
• Institute of Electrical and Electronics Engineers, Inc. (IEEE)
• The Japan Society of Mechanical Engineers (JSME)
• The Robotics Society of Japan (RSJ)
• The Japanese Society of Instrumentation and Control Engineers (SICE)

Name:
Taketoshi Mishima

Affiliation:
Professor, Graduate School of Science and Engineering, Saitama University

Address:
255 Shimo-Okubo, Sakura-ku, Saitama-shi, Saitama 338-8570, Japan

Brief Biographical History:
1974- Research Scientist of ETL (Electrotechnical Laboratory, AIST, MITI)
1979- Senior Research Scientist of ETL (Electrotechnical Laboratory, AIST, MITI)
1995- Professor of Information and Computer Science at Saitama University

Main Works:
• K. Kawabata, S. Morishita, H. Takemura, K. Hotta, T. Mishima, H. Asama, H. Mizoguchi, and H. Takahashi, "Development of an Automated Microscope for Supporting Qualitative Asbestos Analysis by Dispersion Staining," J. of Robotics and Mechatronics (JRM), Vol.21, No.2, pp. 186-192, 2009.

Membership in Academic Societies:
• Mathematical Society of Japan (MSJ)
• Information Processing Society of Japan (IPSJ)
• The Institute of the Electronics, Information and Communication Engineers (IEICE)

Name:
Hiroshi Mizoguchi

Affiliation:
Department of Mechanical Engineering, Faculty of Science and Technology, Tokyo University of Science

Address:
2641 Yamazaki, Noda, Chiba 278-8510, Japan

Brief Biographical History:
1985- Research & Development Center, TOSHIBA Corp.
1994- Research Center for Advanced Science and Technology, The University of Tokyo
1997- Department of Information and Computer Science, Saitama University
2002- Department of Mechanical Engineering, Tokyo University of Science

Main Works:
• Y. Sasaki, S. Kagami, and H. Mizoguchi, "Online Short Term Multiple Sound Source Mapping for a Mobile Robot by Robust Motion Triangulation," Advanced Robotics, Vol.23, No.1-2, pp. 145-164, 2009.

Membership in Academic Societies:
• The Institute of Electrical and Electronics Engineers (IEEE)
• The Japan Society of Mechanical Engineers (JSME)
• The Robotics Society of Japan (RSJ)